ADVANCED FUNCTIONAL MATERIALS
www.afm-journal.de

Origin of Reduced Bimolecular Recombination in Blends of Conjugated Polymers and Fullerenes

*D. H. K. Murthy, Armantas Melianas, Zheng Tang, Gytis Juška, Kęstutis Arlauskas, Fengling Zhang, Laurens D. A. Siebbeles, Olle Inganäs, and Tom J. Savenije**

Bimolecular charge carrier recombination in blends of a conjugated copolymer based on a thiophene and quinoxaline (TQ1) with a fullerene derivative ((6,6)-phenyl-C_{71}-butyric acidmethyl ester, $PC_{71}BM$) is studied by two complementary techniques. TRMC (time-resolved microwave conductance) monitors the conductance of photogenerated mobile charge carriers locally on a timescale of nanoseconds, while using photo-CELIV (charge extraction by linearly increasing voltage) charge carrier dynamics are monitored on a macroscopic scale and over tens of microseconds. Despite these significant differences in the length and time scales, both techniques show a reduced Langevin recombination with a prefactor ζ close to 0.05. For TQ1:$PC_{71}BM$ blends, the ζ value is independent of temperature. On comparing TRMC data with electroluminescence measurements it is concluded that the encounter complex and the charge transfer state have very similar energetic properties. The ζ value for annealed poly(3-hexylthiophene) (P3HT):(6,6)-phenyl-C_{61}-butyric acid methyl ester ($PC_{61}BM$) is approximately 10^{-4}, while for blend systems containing an amorphous polymer ζ values are close to 1. These large differences can be related to the extent of charge delocalization of opposite charges in an encounter complex. Insight is provided into factors governing the bimolecular recombination process, which forms a major loss mechanism limiting the efficiency of polymer solar cells.

1. Introduction

The efficient conversion of photons into free charge carriers in blends of conjugated polymers and fullerene derivatives is quite promising for the development of bulk heterojunction (BHJ) solar cells. The power conversion efficiency (PCE) of BHJ solar cells has significantly improved from 2.5% to more than 9.5% over the last decade.[1] This enhancement can be partly attributed to the use of low band-gap conjugated polymers to extend the spectral absorption into the NIR region and to the advance of the nanomorphology of the BHJ to improve the charge generation and transport. Further enhancement in the PCE can be achieved by minimizing geminate and bimolecular (or non-geminate) recombination of charge carriers. Particularly, bimolecular recombination is shown to strongly affect the fill factor[2] and the V_{oc}[3] that crucially influences the PCE.[4]

Charge formation in a BHJ blend starts by the absorption of a photon yielding a bound electron/hole pair or exciton. The dissociation of the exciton at the polymer fullerene interface results in a charge transfer state (CT state) in which an electron resides on the fullerene and a hole on the polymer at a limited distance. In principle, these Coulombically bound states should overcome their mutual attraction to form free charge carriers. Recently, we showed that delocalization of the charges in the CT state lowers the Coulombic binding energy between the opposite charges, assisting the separation resulting in the formation of mobile charges.[5] In BHJ solar cells these free charges can undergo bimolecular recombination forming a major loss mechanism. Over the last years, the Langevin theory[6] has been used to describe the recombination of charge carriers in organic semiconductors such as conjugated polymers. The Langevin recombination rate (β_L) is given by Equation 1,

D. H. K. Murthy, Prof. L. D. A. Siebbeles,
Dr. T. J. Savenije
Optoelectronic Materials Section
Department of Chemical Engineering
Delft University of Technology
2628 BL Delft, The Netherlands
E-mail: T.J.Savenije@tudelft.nl
D. H. K. Murthy
Dutch Polymer Institute (DPI)
P.O. Box 902, 5600 AX Eindhoven, The Netherlands.

A. Melianas, Z. Tang, Dr. F. Zhang, Prof. O. Inganäs
Department of Physics
Chemistry and Biology
Biomolecular and Organic Electronics
Center of Organic Electronics (COE)
Linkoping University
58183 Linkoping, Sweden
Prof. K. Arlauskas, Prof. G. Juška
Department of Solid State Electronics
Vilnius University
10222 Vilnius, Lithuania

DOI: 10.1002/adfm.201203852

$$\beta_L = \frac{e(\mu_e + \mu_h)}{\varepsilon\varepsilon_0} \quad (1)$$

where e is the elementary charge, μ_e and μ_h are the electron and hole mobilities and ε, ε_o are the relative and absolute dielectric permittivity, respectively.

For a number of BHJ blends the observed experimental bimolecular recombination rate (β_{exp}) of charge carriers can indeed be described by Equation 1.[7] However, a number of polymer blends, i.e., annealed poly(3-hexylthiophene)(P3HT):phenyl-C_{61}-butyric acid methyl ester (PCBM), poly[(4,4′-bis(2-ethylhexyl) dithieno[3,2-b:2′,3′-d]silole)-2,6-diyl-alt-(4,7-bis(2-thienyl)-2,1,3-benzothiadiazole)-5,5′-diyl] (Si-PCPDTBT):PCBM and poly[4,4′-bis(2-ethylhexyl)dithieno[3,2-b:2′,3′-d]silole)-2,6-diyl-alt-(2,5-bis(3-tetradecylthiophen-2-yl)thiazolo-5,4-d-thiazole)-2,5-diyl] (KP115):PCBM exhibit two to four orders smaller β_{exp} values as compared to β_L.[8] The ratio between β_{exp}/β_L is referred in literature as the Langevin prefactor, ζ. Several models to explain this reduced-Langevin recombination behavior are reported: Österbacka et al.[8a] attributed the reduced-Langevin recombination to 2D recombination in the lamellar structure of conjugated polymer. Deibel et al. proposed that a gradient in the carrier-concentration within a device is the reason for reduced-Langevin recombination,[8b] while according to Szmytkowski[8c] it is the difference in the local dielectric constant. Furthermore, Koster et al.[9] proposed that bimolecular recombination is predominantly governed by the slowest charge carrier instead of the fastest one. Nevertheless, despite these research efforts, the basis for observing reduced-Langevin recombination is unclear and it is crucial to get better insight on this process to improve the PCE of organic solar cells.

In this work, we investigate the charge carrier recombination process in blends of TQ1 with phenyl-C_{71}-butyric acid methyl ester ($PC_{71}BM$) by employing the microwave photoconductance technique (TRMC) and photogenerated charge extraction by linearly increasing voltage (photo-CELIV) techniques. The TRMC monitors the conductance of photogenerated mobile charge carriers locally (microscopic) on a timescale of nanoseconds, while the photo-CELIV monitors charge carrier dynamics on a macroscopic scale and on much longer timescales. Note that both techniques provide information on the recombination processes close to those observed under open circuit conditions. The TQ1:$PC_{71}BM$ ratio and the thickness of the photoactive layer are kept constant for both experiments to allow comparison of the results of both techniques. For the TRMC measurements the temperature was varied between 220 and 300 K and in addition, the laser intensity was varied over a factor of 30. The TRMC traces were fitted to obtain the charge carrier mobilities and β_{exp} from which the prefactor ζ is deduced. Next, the recombination dynamics and charge carrier mobilities from the photo-CELIV experiments are discussed and again the prefactor ζ is derived. Interestingly, the prefactor as determined by both techniques are found to be very close. A kinetic scheme is presented to explain the physical origin of the prefactor.

2. Results and Discussion

Figure 1 shows microwave photoconductance transients (dotted lines) recorded using different incident intensities varying over a factor of 30. On photoexcitation of the blend layer with a 3.5 ns laser pulse, the transient shows a clear rise followed by a slow decay on a time scale of hundreds of nanoseconds. Due to the 18 ns response time of the microwave cavity the maximum of the photoconductance signal is observed at about 30 ns. As no electrodes are involved in TRMC measurements, the conductance decay is merely due to recombination of mobile charge carriers or trapping.[10]

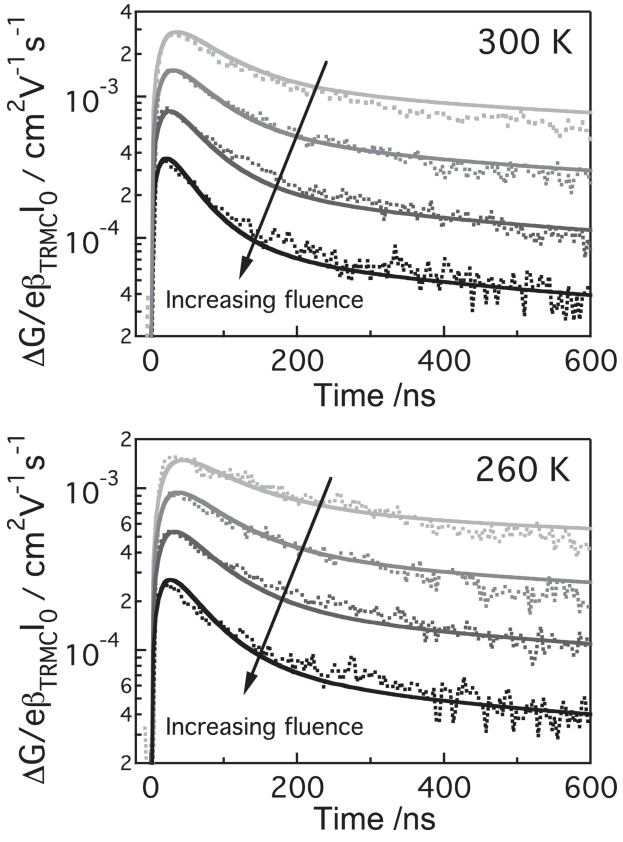

Figure 1. Photoconductance traces (dotted) normalized to the incident laser fluence for TQ1:$PC_{71}BM$ at indicated temperatures on varying the fluence from 1.5×10^{12} photons cm^{-2} to 5×10^{13} photons cm^{-2} using a wavelength of 612 nm. The solid lines are fits to the data points according to the kinetics shown in Scheme 1.

On comparing the decay dynamics of the photoconductance traces obtained at 260 and 300 K shown in Figure 1, it is clear that the decay becomes faster at higher temperatures (see Supporting Information Figure S1). Similar observations were previously reported for P3HT:$PC_{61}BM$ blends.[11] In addition, it can be noticed that the maximum change in photoconductance increases with higher temperatures. As argued for P3HT:$PC_{61}BM$ blends this rise can be attributed to higher electron mobility on the fullerenes, and hole mobility on the polymer, while the yield of charges was found to be temperature independent.[11] For the present blends the activation energies are similar to those found for P3HT:$PC_{61}BM$ (see Supporting Information Figure S2) indicating again the yield remains constant with temperature.

To determine the bimolecular recombination rate, β_{exp}, the TRMC traces were fitted using a routine based on the

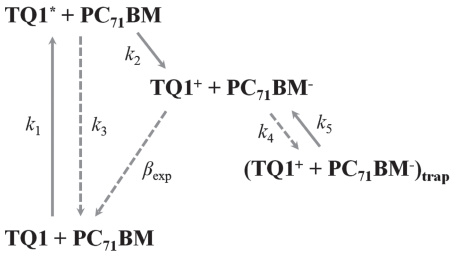

k_1 : photo-excitation
k_2 : exciton dissociation
k_3 : exciton hole recombination
k_4 : charge trapping
k_5 : charge release
β_{exp} : bimolecular charge recombination

Scheme 1. Summary of the photophysical processes occurring on photoexcitation of the TQ1:$PC_{71}BM$ blend. k_3 is the bimolecular recombination rate constant for the decay of an excited state with a positive charge, resulting in the decay of the excited state while the concentration of holes is unaltered. The rate constant β_{exp} represents bimolecular (non-geminate) recombination of mobile charges.

photophysical model as detailed in **Scheme 1**. In short, photoexcitation of the blend (k_1) is determined by the temporal profile and intensity of the laser in combination with the optical absorption of the blend at the wavelength used. Charge formation (k_2) is assumed to be a fast (multiple) process as compared to the width of the laser pulse, with a fixed rate constant. Exciton-hole recombination (k_3) that has been reported previously to occur in blends[12] is a bimolecular process resulting in the decay of an excited state, however not affecting the concentration of the holes. This process has to be taken into account if light fluences are substantially higher than 1 sun, like in the TRMC experiments. Formation of a strongly bound charge transfer state, followed by geminate recombination could occur, however these intermediates do not contribute to the measured photoconductance signal. First order trapping (k_4) and thermal release (k_5) of charge carriers are also included, which is more pronounced at low temperatures. Apart from energetic trapping, this process (k_4) also takes into account the diffusion of charges to more amorphous areas, which are characterized by a low mobility. Finally, the rate constant β_{exp}, represents the bimolecular recombination between mobile electrons and holes. Note that both charges $TQ1^+$ and $PC_{71}BM^-$ are expected to be mobile (see Supporting Information Figure S2) and hence they both contribute to the photoconductance. Since the TRMC technique is not capable of discriminating between positive and negative charge carriers, in the fit routine all generated charge carriers obtain a total mobility of ($\mu_e + \mu_h$) except for those charges that are trapped and are hence immobile. Note that TRMC experiments are performed under low electric filed strengths. The rate constants found might be different in solar cells operating at maximum power point. As shown in Figure 1 (solid lines) reasonable good fits are obtained for the observed traces at various incident intensities for one set of kinetic parameters using this relatively simple scheme. There is no need to assume concentration dependent bimolecular recombination rates. The Supporting Information contains more details regarding the fit procedure including the rate constants found at various temperatures.

The values of β_{exp} determined using the above fitting method are plotted in **Figure 2** versus temperature. A clear rise of the recombination rate is observed on increasing the temperature from 220 to 300 K. Furthermore the Langevin recombination rates, β_L, are calculated using the total mobility of ($\mu_e + \mu_h$) as obtained from the fitting routine and using Equation 1. These values are shown in Figure 2. The β_{exp} values are approximately two orders of magnitude smaller as compared to β_L, implying the β_{exp} rates are reduced. The prefactor ζ, determined by the ratio β_{exp}/β_L, is found to be ≈0.05 and independent of temperature from 220 K to 300 K within the experimental error. For annealed P3HT:PCBM a prefactor of 1×10^{-4} has been determined at room temperature using a similar approach.[13] Most importantly, the clear proportionality between β_{exp} and β_L indicates that these experimentally obtained parameters are physically related, and that the size of the prefactor ζ is related to the nature of the encounter complex. The physical origin of reduced bimolecular recombination is discussed later in this section.

Figure 3 shows the charge carrier density n decay deduced by photo-CELIV experiments in the microsecond regime. Note that in this case a complete solar cell is measured, instead of TQ1:$PC_{71}BM$ film without electrodes as in the TRMC experiment. The charge carrier mobility estimated by photo-CELIV is approximately $\mu = 2 \times 10^{-4}$ cm^2 V^{-1} s^{-1}. This corresponds to β_L values of 1×10^{-10} cm^3 s^{-1} according to Equation 1. By varying the time delay, t_{delay}, between the short laser pulse and

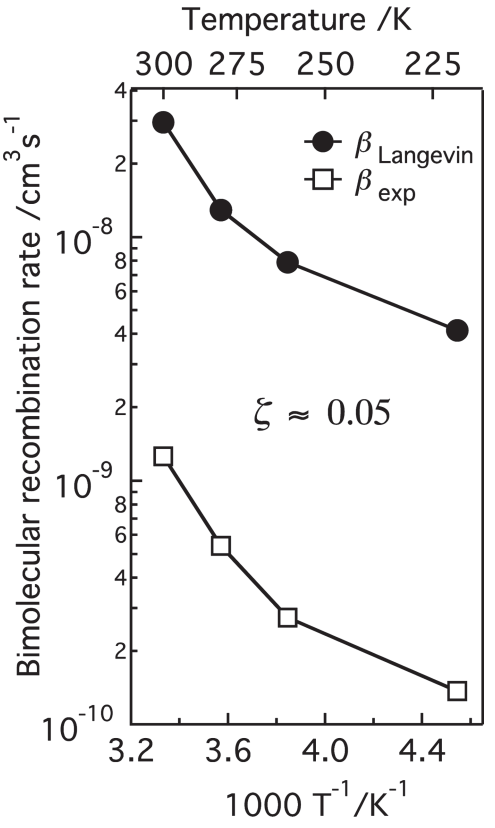

Figure 2. Effect of temperature on the bimolecular recombination rate: β_{exp} values are determined by fitting the decays at various temperatures and the Langevin rate (β_L) is calculated according to Equation 1, using the mobility values found from the fitting routine.

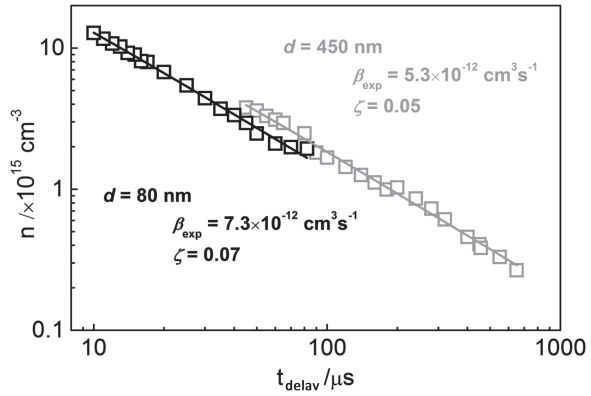

Figure 3. Extracted charge-carrier density, *n*, as a function of delay time deduced by photo-CELIV at room temperature. Two solar cells of different active layer thickness, *d*, are measured (black *d* = 80, grey *d* = 450 nm). Black trace corresponds to the same active layer as in TRMC measurements. Solid lines are fits of the data to a bimolecular decay.

the linearly increasing extraction voltage ramp, charge carrier recombination kinetics on a microsecond time scale can be examined. In Figure 3 the slope of *n* versus t_{delay} is –1, which allows us to fit the data to a bimolecular decay (see Experimental Section). The bimolecular recombination rate, β_{exp}, is found to be 7.3×10^{-12} cm^3 s^{-1} (Figure 3 black), which is comparable to those reported for P3HT:PCBM based solar cells.[14] To observe charge carrier recombination at even longer time delays (Figure 3 grey) a solar cell with a thicker active layer *d* = 450 nm was measured (see Supporting Information). The estimated bimolecular recombination rate $\beta_{exp} = 5.3 \times 10^{-12}$ cm^3 s^{-1} and the Langevin prefactor $\zeta = 0.05$ are, within experimental error, in excellent agreement in both samples. In fact, the two plots of Figure 3 can be considered as one, spanning the time range from 10 to 650 μs.

Most importantly the reduction factor, ζ, obtained by photo-CELIV, is found to be ≈0.05 in agreement with the TRMC results discussed above. Note that, despite different measurement principles of probing charge carrier dynamics, both TRMC and photo-CELIV show reduced bimolecular recombination with similar values for ζ. This issue including the substantial differences observed in charge carrier mobility using both techniques will be addressed at the end of this section.

In the following part, we try to understand the physical origin of the reduced bimolecular recombination. As has been reported recently and depicted in **Scheme 2**, the Langevin rate, β_L denotes the rate for mobile charge carriers to form a so-called encounter complex.[13,15] This complex can either undergo recombination to the ground state or dissociate back into mobile charges, depending on the rate constants k_r and k_d. We relate the prefactor ζ to the properties of the encounter complex by assuming that $\zeta = k_r/k_d$. In case of reduced bimolecular recombination: $k_d > k_r$. For TQ1:PC$_{71}$BM blends a value for ζ of ≈0.05 implies that recombination to the ground state occurs only one out of approximately twenty times an encounter complex is formed. Furthermore, the ζ value for annealed P3HT:PC$_{61}$BM is approximately 10^{-4}[13] i.e., two orders smaller than found for TQ1:PC$_{71}$BM. This implies that a complex formed in a P3HT:PC$_{61}$BM blend has an approximately 100 times higher chance to dissociate into free charges than a complex formed in TQ1:PC$_{71}$BM. To explain this large difference, the ζ values might tentatively be related to the extent of charge delocalization of opposite charges in an encounter complex. As has been suggested previously by theoretical modeling, delocalization reduces the binding energy between the charges[16] enhancing the possibility for a complex to dissociate. On comparing the morphology of the polymer constituents in both blends, it can be concluded that the crystalline P3HT is more ordered than TQ1, which is liquid crystalline at best.[17] The high crystallinity of P3HT might result in a more extensive charge delocalization of the positive charge carrier in the polymer domains. This results in a higher chance for the complex to dissociate, and hence a smaller ζ values for P3HT:PC$_{61}$BM in comparison to TQ1:PC$_{71}$BM.

To substantiate our model we collected the reported recombination rates for a number of blends by examining existing literature. The bimolecular recombination rate found in blends consisting of an amorphous polymer such as poly[2,6-(4,4-bis-(2-ethylhexyl)-4H-cyclopenta[2,1-b:3,4-b′]-dithiophene)-alt-4,7-(2,1,3-benzothiadiazole)] (PCPDTBT),[15] poly[2-methoxy-5-(3′,7′-demethyloctyloxy)-1,4-phenylenevinylene] (MDMO-PPV),[18] poly[[9-(1-octylnony)-9H-carbazole-2,7-diyl]-2,5-thiophenediyl-2,1,3-benzothiadiazole-4,7-diyl-2,5-thiophnediyl] (PCDTBT),[19] regiorandom P3HT,[4b,7] are close to values predicted by Langevin recombination theory, i.e., ζ values are close to 1. However, blends containing polymers, such as silicon substituted PCPDTBT,[8f] fluorine substituted PCPDTBT,[20] silole based polymers (KP115)[8d] and annealed P3HT[21] exhibited a reduced bimolecular recombination rate. Interestingly, the latter set of polymers has a common feature: improved planarity of the polymer backbone and better π–π stacking leading to a well-ordered nanomorphology.[22] The enhancement in the ordering nature of the polymer allows delocalization of the charge carriers, which positively affects the dissociation rate, k_d of the encounter complex and hence results in a reduced bimolecular recombination.

A striking question now is whether this encounter complex has similar properties as the CT state formed on optical excitation of a blend. More specifically: Is the binding energy between opposite charges in each of these complexes equal? If the complexes have similar properties the photon energy required to excite an electron from the highest occupied molecular orbital (HOMO) of the TQ1 to the lowest unoccupied molecular orbital (LUMO) of PC$_{71}$BM (k_{CT} in Scheme 2) should match the energy of the luminescence corresponding to the radiative decay of an encounter complex to the ground state. The latter could be

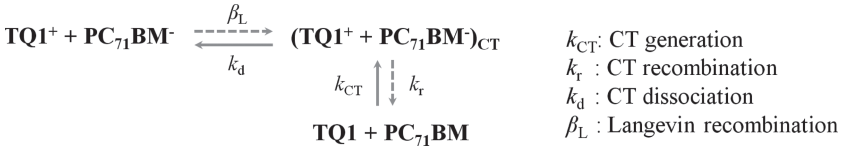

Scheme 2. Kinetic processes involved in bimolecular recombination based on the scheme. The Langevin rate β_L defines the rate for mobile opposite charge carriers to form an encounter complex. This encounter complex can decay to the ground state (k_r) or dissociate back into mobile charges (k_d).

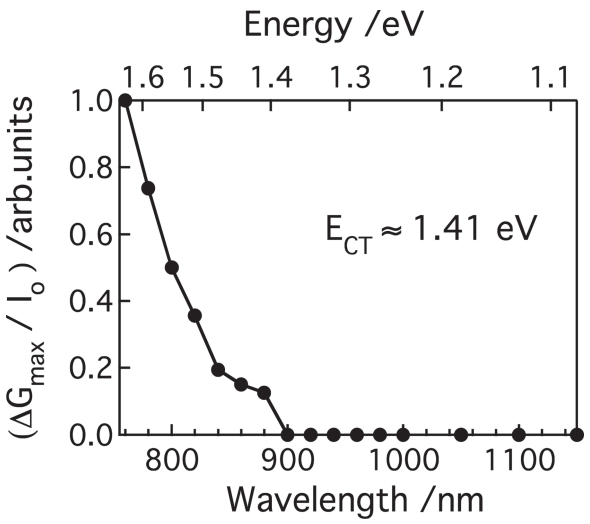

Figure 4. Intensity normalized photoconductance action spectrum for a blend of TQ1 with $PC_{71}BM$.

measured by electroluminescence (EL) and is found to amount to ≈1.4 eV.[23] Hence optical excitation at this wavelength should result in the promotion of an electron from the HOMO of the polymer directly to the LUMO of the fullerene, yielding the CT state. **Figure 4** shows a TRMC action spectrum where the maximum photoconductance values normalized to the incident intensity ($\Delta G_{max}/I_0$) are plotted as function of the excitation wavelength. Interestingly, when exciting at 1.41 eV, where neither TQ1 nor $PC_{71}BM$ absorbs, formation of mobile charge carriers is observed. From the onset in the TRMC action spectrum it is inferred that the energy of the CT state amounts to ≈1.41 eV. In addition, the energy of the CT state deduced from the Fourier-transform photocurrent spectroscopy (FTPS) technique was found to be ≈1.45 eV.[24] From these observations it can be concluded that the energetic properties of the encounter complex and the CT state for TQ1:$PC_{71}BM$ are identical. For annealed blends of P3HT:$PC_{61}BM$ the energies found using EL and TRMC match perfectly, again indicating that the encounter complex is similar in nature as the CT state.[25] These observations suggest that bimolecular recombination occurs via an intermediate resembling the CT state.

Finally we address the question why both techniques giving such different values for the charge carrier mobility, however still yield comparable ζ values. As mentioned above, both techniques probe at different times and length scales.[26] Identical to recent THz measurements on TQ1:PCBM,[27] using TRMC the highly mobile charges are predominantly probed. These mobile charges rapidly face a counter charge to form an encounter complex. Thus if ($\mu_e + \mu_h$) is high, also the bimolecular recombination rate, β_{exp}, is high. With photo-CELIV, apart from mobile charges, also charges that have (for some period) been immobilized due to trapping are measured. This implies that the observed mean mobility of the carriers is substantially lower than measured with TRMC. However, as parts of these charges have been immobilized,[26] bimolecular recombination is reduced accordingly. Despite the differences in the measured ($\mu_e + \mu_h$) and β_{exp}, the observed ζ values obtained by both photo-CELIV and TRMC are equal as ζ depends mostly on the nature of the encounter complex. Also, from above considerations we can deduce that for a specific blend the ζ value is independent of the mobility. This conclusion is supported by our temperature dependent TRMC measurements: By changing the temperature the mobility is in fact varied, however the ζ is constant (see Figure 2), In view of the kinetics shown in Scheme 2 a constant ζ value means that the ratio between k_r and k_d remains constant, which implies that either both rate constants stay the same or both rate constants are in the same way dependent on the mobility of the charge carriers. As it is not directly evident how k_r should be affected by the mobility we suggest that both k_r and k_d are independent of the mobility. This is also in line with our previous arguments that k_d is predominantly affected by charge delocalization.

3. Conclusions

We have investigated charge carrier recombination processes in TQ1:$PC_{71}BM$ blends by using the TRMC and photo-CELIV techniques. TRMC monitors the conductance of photogenerated mobile charge carriers locally while using photo-CELIV charge carrier dynamics are monitored on a macroscopic scale. Despite the significant differences in the spatial and temporal scales involved in both techniques, a reduced bimolecular recombination with a prefactor, ζ, close to 0.05 is observed. Temperature dependent TRMC measurements indicate a clear proportionality between experimentally measured β_L and β_{exp}, suggesting that the size of the prefactor ζ is related to the nature of the encounter complex. The prefactor ζ can be described by the ratio between the rate constants for recombination of the encounter complex back to the ground state (k_r) and for dissociation forming mobile charges again (k_d). From the TRMC action spectra and electroluminescence measurements it can be concluded that both the encounter complex and the CT state have identical energetic properties for TQ1:$PC_{71}BM$ blends, which is also true for P3HT:$PC_{61}BM$ blends. These observations suggest that bimolecular recombination occurs via an intermediate resembling the CT state.

For blend systems, containing an amorphous polymer ζ values close to 1 have been observed. The ζ value for annealed P3HT:$PC_{61}BM$ is much smaller, approximately 10^{-4},[13] i.e., two orders smaller than found for TQ1:$PC_{71}BM$. These large differences between the ζ values can be related to the extent of charge delocalization of opposite charges in an encounter complex. The enhancement in the ordering nature of the polymer allows delocalization of the charge carriers, which is expected to reduce the binding energy between them, enhancing the dissociation rate k_d of the encounter complex. The higher possibility for a complex to dissociate leads to smaller ζ values. Thus, inducing the ordering of the conjugated polymer in addition to fullerene segregation seems like a prerequisite to achieve reduced bimolecular recombination.

4. Experimental Section

In this work, a blend of a low band gap conjugated polymer based on thiophene and quinoxaline named as poly[2,3-bis-(3-octyloxyphenyl)

quinoxaline-5,8-diyl-alt-thiophene-2,5-diyl] (TQ1) with a fullerene derivative, $PC_{71}BM$ was used. The blend solution of TQ1 with $PC_{71}BM$ (1:2.5 weight ratio) was prepared using ortho-dichlorobenzene solvent. The thickness of the photoactive layer was ≈80 nm. This blend composition has previously demonstrated 6% PCE with a remarkably high 0.9 V open circuit voltage. Reports on the synthesis of the TQ1, optical, morphological and electrical properties of TQ1:$PC_{71}BM$ blend are detailed by Wang et al.[28]

TRMC: The TRMC technique was employed to investigate the formation of mobile charge carriers and their decay with time. In using this technique, the change in conductance of the film, on photoexcitation was recorded on a nanosecond time scale without applying external electrodes. Temperature dependent TRMC measurements were carried out using a custom-made liquid nitrogen cooled microwave cavity with a resonance frequency at ca. 8.45 GHz. Samples were photoexcited with a 3 ns laser pulse from an optical parametric oscillator pumped at 355 nm with the third harmonic of a Q-switched Nd:YAG laser (Vibrant II, Opotek). Photogeneration of mobile charge carriers in the sample leads to an increase of the conductance, $\Delta G(t)$, and consequently to an enhanced absorption of microwave power by the sample. The time-dependent change of the conductance is obtained from the normalized change in microwave power ($\Delta P(t)/P$) reflected from the cavity according to

$$\frac{\Delta P(t)}{P} = -\ K \Delta G(t) \tag{2}$$

The geometrical dimensions of the cavity and dielectric properties of the media in the microwave cavity determine the sensitivity factor, *K*. From the maximum change in the conductance (ΔG_{max}) and the incident light (I_0), the parameter $\eta\Sigma\mu$ denoting the product of the charge carrier generation yield (η) per incident photon and the sum of the electron and hole mobilities ($\Sigma\mu$) can be calculated using

$$\eta\Sigma\mu = \frac{\Delta G_{max}}{I_0 \beta_{TRMC}\, e} \tag{3}$$

where β_{TRMC} is the ratio between the broad and narrow inner dimensions of the waveguide and *e* is the elementary charge. For more experimental details see references.[29]

Photo-CELIV: The photo–CELIV technique was employed to study charge carrier transport and recombination on a μs time scale. Charge carriers were generated by a 3 ns laser pulse from an optical parametric oscillator (GWU VersaScan/120MB) pumped at 355 nm with the third harmonic of a Q-switched Nd:YAG laser (New Wave Research, Tempest 10). The excitation wavelength was 500 nm. After a time delay, t_{delay}, photogenerated charge carriers were extracted by a linearly increasing voltage, applied by a digital function generator (Stanford Research DS 345). The solar cell was kept at a constant offset voltage (close to V_{oc}) prior to extraction to avoid photogenerated charge carrier leakage out of the device. However, applied constant offset voltage, U_{off}, could lead to charge carrier injection to the active layer from the electrodes, which may have affected the experimental results. Thus, U_{off} was chosen so that both the photogenerated charge carrier leakage and the injection current would be minimal (See Supporting Information for further discussion). Transients were recorded by a digital storage oscilloscope (Tektronix TDS 220).

Semitransparent solar cells in inverted geometry with the following structure: ITO/PFPA–1/TQ1:$PC_{71}BM$/PEDOT:PSS PH1000 were measured (see Supporting Information Figure S4 for device characteristics). Active layer fabrication was identical to that used for TRMC sample preparation, leading to the same active layer thickness, morphology etc. For more details on sample fabrication, device parameters etc. see ref. [30].

Charge carrier mobility was estimated from the temporal position of the extraction current maximum, t_{max}, which largely depends on the experimental conditions.[31] The formula used for the calculations is dependent on the approximation method employed. In this work charge carrier mobility is estimated as suggested by Juška et al.[32]

$$\mu = \frac{2}{3}\frac{d^2}{A t_{max}^2}\frac{1}{1 + 0.36\frac{\Delta j}{j_0}} \tag{4}$$

where *A* is the voltage ramp speed, *d* is the sample thickness, Δj is the maximum extraction current, j_0 is the initial current. For more detailed information see ref. [31,32].

Charge carrier recombination was studied by varying the time delay between the short laser pulse and the linearly increasing voltage. Firstly, a CELIV transient in the dark was measured as a reference. Photo-CELIV transients at different time delays were then recorded. By subtracting the reference CELIV transient from the photo–CELIV transients and integrating the resulting data, extracted charge as a function of time delay was obtained. Charge carrier concentration, *n*, was obtained by dividing the extracted charge by the volume of the active layer. The resulting plots of *n* versus t_{delay} were fitted to a power law in a log-log plot. The differential equation for bimolecular recombination:

$$\frac{dn}{dt} = -\ \beta_{exp} n^2 \tag{5}$$

has the general solution (assuming concentration independent β_{exp}):

$$n(t) = \frac{1}{\beta_{exp} t + 1/n(0)} \tag{6}$$

which has a slope of –1 in a log-log plot. We find our power law fits to also have a slope of –1. Hence the data points could be fitted using Equation (5). The obtained charge carrier mobility and bimolecular recombination values were then used to calculate the Langevin prefactor, ζ.

Supporting Information

Supporting Information is available from the Wiley Online Library or from the author.

Acknowledgements

The work of D.H.K.M. forms the research program of the Dutch Polymer Institute (DPI, project #681). Research on organic photovoltaics at Linköping University was financed by the Swedish Energy Agency. Research at Vilnius University was funded by the European Social Fund under the Global Grant measure. The authors gratefully acknowledge the synthesis of polymers by Dr. Ergang Wang and Prof. Mats Andersson, Chalmers University of Technology, and discussions with L. Mattias Andersson, Lund University.

Received: December 27, 2012
Revised: February 12, 2013
Published online: April 2, 2013

[1] a) L. T. Dou, J. B. You, J. Yang, C. C. Chen, Y. J. He, S. Murase, T. Moriarty, K. Emery, G. Li, Y. Yang, *Nat. Photonics* **2012**, *6*, 180; b) M. A. Green, K. Emery, Y. Hishikawa, W. Warta, E. D. Dunlop, *Prog. Photovolt: Res. Appl.* **2012**, *20*, 12; c) R. F. Service, *Science* **2011**, *332*, 293.

[2] R. Mauer, I. A. Howard, F. Laquai, *J. Phys. Chem. Lett.* **2010**, *1*, 3500.

[3] D. Credgington, R. Hamilton, P. Atienzar, J. Nelson, J. R. Durrant, *Adv. Funct. Mater.* **2011**, *21*, 2744.

[4] a) A. Pivrikas, H. Neugebauer, N. S. Sariciftci, *IEEE J. Sel. Top. Quantum Electron.* **2010**, *16*, 1746; b) A. Pivrikas, N. S. Sariciftci, G. Juska, R. Osterbacka, *Prog. Photovolt: Res. Appl.* **2007**, *15*, 677; c) P. E. Keivanidis, V. Kamm, W. M. Zhang, G. Floudas, F. Laquai, I. McCulloch, D. D. C. Bradley, J. Nelson, *Adv. Funct. Mater.* **2012**, *22*, 2318.

[5] D. H. K. Murthy, M. Gao, M. J. W. Vermeulen, L. D. A. Siebbeles, T. J. Savenije, *J. Phys. Chem. C* **2012**, *116*, 9214.
[6] P. Langevin, *Ann. Chim. Phys.* **1903**, *28*, 433.
[7] A. Pivrikas, R. Osterbacka, G. Juska, K. Arlauskas, H. Stubb, *Synth. Met.* **2005**, *155*, 242.
[8] a) R. Osterbacka, A. Pivrikas, G. Juska, A. Poskus, H. Aarnio, G. Sliauzys, K. Genevicius, K. Arlauskas, N. S. Sariciftci, *IEEE J. Sel. Top. Quantum Electron.* **2010**, *16*, 1738; b) C. Deibel, A. Wagenpfahl, V. Dyakonov, *Phys. Rev. B* **2009**, *80*, 075203; c) J. Szmytkowski, *Chem. Phys. Lett.* **2009**, *470*, 123; d) T. M. Clarke, J. Peet, P. Denk, G. Dennler, C. Lungenschmied, A. J. Mozer, *Energy Environ. Sci.* **2012**, *5*, 5241; e) A. Pivrikas, G. Juska, A. J. Mozer, M. Scharber, K. Arlauskas, N. S. Sariciftci, H. Stubb, R. Osterbacka, *Phys. Rev. Lett.* **2005**, *94*, 176806; f) M. C. Scharber, M. Koppe, J. Gao, F. Cordella, M. A. Loi, P. Denk, M. Morana, H. J. Egelhaaf, K. Forberich, G. Dennler, R. Gaudiana, D. Waller, Z. G. Zhu, X. B. Shi, C. J. Brabec, *Adv. Mater.* **2010**, *22*, 367; g) T. M. Clarke, D. B. Rodovsky, A. A. Herzing, J. Peet, G. Dennler, D. DeLongchamp, C. Lungenschmied, A. J. Mozer, *Adv. Energy Mater.* **2011**, *1*, 1062.
[9] L. J. A. Koster, V. D. Mihailetchi, P. W. M. Blom, *Appl. Phys. Lett.* **2006**, *88*, 052104.
[10] T. J. Savenije, D. H. K. Murthy, M. Gunz, J. Gorenflot, L. D. A. Siebbeles, V. Dyakonov, C. Deibel, *J. Phys. Chem. Lett.* **2011**, *2*, 1368.
[11] W. J. Grzegorczyk, T. J. Savenije, T. E. Dykstra, J. Piris, J. M. Schins, L. D. A. Siebbeles, *J. Phys. Chem. C* **2010**, *114*, 5182.
[12] a) J. M. Hodgkiss, S. Albert-Seifried, A. Rao, A. J. Barker, A. R. Campbell, R. A. Marsh, R. H. Friend, *Adv. Funct. Mater.* **2012**, *22*, 1567; b) A. J. Ferguson, N. Kopidakis, S. E. Shaheen, G. Rumbles, *J. Phys. Chem. C* **2008**, *112*, 9865.
[13] A. J. Ferguson, N. Kopidakis, S. E. Shaheen, G. Rumbles, *J. Phys. Chem. C* **2011**, *115*, 23134.
[14] G. Juska, G. Sliauzys, K. Genevicius, K. Arlauskas, A. Pivrikas, M. Scharber, G. Dennler, N. S. Sariciftci, R. Osterbacka, *Phys. Rev. B* **2006**, *74*, 115314.
[15] S. Yamamoto, H. Ohkita, H. Benten, S. Ito, *J. Phys. Chem. C* **2012**, *116*, 14804.
[16] C. Deibel, T. Strobel, V. Dyakonov, *Phys. Rev. Lett.* **2009**, *103*, 036402.
[17] E. Wang, J. Bergqvist, K. Vandewal, Z. Ma, L. Hou, A. Lundin, S. Himmelberger, A. Salleo, C. Müller, O. Inganäs, F. Zhang, M. R. Andersson, *Adv. Energy Mater.* DOI:10.1002/aenm.201201019.
[18] G. Dennler, A. J. Mozer, G. Juska, A. Pivrikas, R. Osterbacka, A. Fuchsbauer, N. S. Sariciftci, *Org. Electron.* **2006**, *7*, 229.
[19] T. M. Clarke, J. Peet, A. Nattestad, N. Drolet, G. Dennler, C. Lungenschmied, M. Leclerc, A. J. Mozer, *Org. Electron.* **2012**, *13*, 2639.
[20] S. Albrecht, S. Janietz, W. Schindler, J. Frisch, J. Kurpiers, J. Kniepert, S. Inal, P. Pingel, K. Fostiropoulos, N. Koch, D. Neher, *J. Am. Chem. Soc.* **2012**, *134*, 14932.
[21] C. Deibel, A. Baumann, V. Dyakonov, *Appl. Phys. Lett.* **2008**, *93*, 163303.
[22] a) S. Subramaniyan, H. Xin, F. S. Kim, S. Shoaee, J. R. Durrant, S. A. Jenekhe, *Adv. Energy Mater.* **2011**, *1*, 854; b) H. J. Son, W. Wang, T. Xu, Y. Y. Liang, Y. E. Wu, G. Li, L. P. Yu, *J. Am. Chem. Soc.* **2011**, *133*, 1885; c) P. Vanlaeke, A. Swinnen, I. Haeldermans, G. Vanhoyland, T. Aernouts, D. Cheyns, C. Deibel, J. D'Haen, P. Heremans, J. Poortmans, J. V. Manca, *Sol. Energy Mater. Sol. Cells* **2006**, *90*, 2150.
[23] Z. Tang, L. M. Andersson, Z. George, K. Vandewal, K. Tvingstedt, P. Heriksson, R. Kroon, M. R. Andersson, O. Inganas, *Adv. Mater.* **2012**, *24*, 554.
[24] K. Vandewal, K. Tvingstedt, O. Inganas, *Phys. Rev. B* **2012**, *86*, 035212.
[25] K. Tvingstedt, K. Vandewal, A. Gadisa, F. L. Zhang, J. Manca, O. Inganas, *J. Am. Chem. Soc.* **2009**, *131*, 11819.
[26] A. Baumann, T. J. Savenije, D. H. K. Murthy, M. Heeney, V. Dyakonov, C. Deibel, *Adv. Funct. Mater.* **2011**, *21*, 1687.
[27] C. S. Ponseca, A. Yartsev, E. Wang, M. R. Andersson, D. Vithanage, V. Sundstrom, *J. Am. Chem. Soc.* **2012**, *134*, 11836.
[28] E. G. Wang, L. T. Hou, Z. Q. Wang, S. Hellstrom, F. L. Zhang, O. Inganas, M. R. Andersson, *Adv. Mater.* **2010**, *22*, 5240.
[29] a) J. E. Kroeze, T. J. Savenije, M. J. W. Vermeulen, J. M. Warman, *J. Phys. Chem. B* **2003**, *107*, 7696; b) A. Huijser, T. J. Savenije, J. E. Kroeze, L. D. A. Siebbeles, *J. Phys. Chem. B* **2005**, *109*, 20166.
[30] Z. Tang, Z. George, Z. Ma, J. Bergqvist, K. Tvingstedt, K. Vandewal, E. Wang, L. M. Andersson, M. R. Andersson, F. Zhang, O. Inganäs, *Adv. Energy Mater.* **2012**, *2*, 1467.
[31] G. Juska, K. Arlauskas, M. Viliunas, K. Genevicius, R. Osterbacka, H. Stubb, *Phys. Rev. B* **2000**, *62*, R16235.
[32] N. Nekrašas, K. Genevicius, M. Viliunas, G. Juška, *Chem. Phys.* **2012**, *404*, 56.